

HYDRODYNAMICS OF THE STREAM-DISK IMPACT IN INTERACTING BINARIES

PHILIP J. ARMITAGE¹ AND MARIO LIVIO
Space Telescope Science Institute, 3700 San Martin Drive, Baltimore, MD 21218;
armitage@cita.utoronto.ca, mlivio@stsci.edu
Draft version November 19, 2018

ABSTRACT

We use hydrodynamic simulations to provide quantitative estimates of the effects of the impact of the accretion stream on disks in interacting binaries. For low accretion rates, efficient radiative cooling of the hotspot region can occur, and the primary consequence of the stream impact is stream overflow toward smaller disk radii. The stream is well described by a ballistic trajectory, but larger masses of gas are swept up and overflow at smaller, but still highly supersonic, velocities. If cooling is inefficient, overflow still occurs, but there is no coherent stream inward of the disk rim. Qualitatively, the resulting structure appears as a bulge extending downstream along the disk rim. We calculate the mass fraction and velocity of the overflowing component as a function of the important system parameters, and discuss the implications of the results for X-ray observations and doppler tomography of cataclysmic variables, low-mass X-ray binaries and supersoft X-ray sources.

Subject headings: accretion, accretion disks — instabilities — hydrodynamics — novae, cataclysmic variables — binaries: general

1. INTRODUCTION

Observations of cataclysmic variables, low-mass X-ray binaries, and supersoft X-ray sources show that accretion disks in these systems display pronounced deviations from axisymmetry, for which the most obvious agent is the impact of the gas stream from the companion star onto the disk (for a review, see e.g. Livio 1993). The complexity of the stream-disk interaction mandates the use of hydrodynamic simulations to fully explore its consequences.

The dynamics of the accretion stream up to the point of impact with the disk was described by Lubow & Shu (1975, 1976). The gas stream leaves the inner Lagrange point in approximate vertical hydrostatic equilibrium, and flows inward along a ballistic trajectory. As it does so, inertia precludes the stream from adjusting fast enough to maintain hydrostatic balance, so that upon reaching the disk edge the stream is substantially more extended vertically than the local hydrostatic value. Gas at several scale heights above the disk midplane may then be able to overflow the disk rim towards smaller disk radii. Some possible observational signatures of this were discussed for X-ray binaries by Frank, King & Lasota (1987), and for cataclysmic variables by Lubow (1989).

In this investigation we extend the study of the stream-disk interaction by performing three dimensional calculations of the stream-disk interaction using the ZEUS hydrodynamics code (Stone & Norman 1992a,b). Our goals are to quantify the degree of stream overflow, to explore the structure of the stream-disk impact region at the disk rim, and to investigate the efficiency of entrainment once the gas stream is overflowing the disk. These theoretical questions correspond closely to observational issues; how much absorption can be generated by an overflowing stream, how extended is the hotspot region, and can the stream-disk impact generate significant emission at velocities intermediate between those of the disk and a ballistic

gas stream?

The layout of this paper is as follows. In §2 we discuss and present the results of hydrodynamic simulations of the stream-disk impact. We compare our results with our previous calculations which used smooth particle hydrodynamics (Armitage & Livio 1996), and with two-dimensional calculations (Rozyczka & Schwarzenberg-Czerny 1987). §3 quantifies the degree of stream overflow as a function of the parameters of the stream and disk, while §4 analyzes the calculated velocity profile of the stream and entrained disk gas. §5 discusses how the simulations compare to current observational results, while §6 summarizes our main conclusions.

2. HYDRODYNAMIC SIMULATIONS OF THE INTERACTION

Hydrodynamic calculations of the interaction of the stream with the accretion disk were carried out with the ZEUS-3D code developed by the Laboratory for Computational Astrophysics (Clarke, Norman & Fiedler 1994). ZEUS-3D is a finite difference code utilizing an artificial viscosity to capture shocks, which has been extensively used and tested for astrophysical fluid dynamics problems. Details of the algorithms used in the code are described by Stone & Norman (1992a, 1992b).

2.1. Initial and boundary conditions

The simulations are performed in Cartesian (x, y, z) geometry, with cubic cells. The computational box surrounds the impact point of the stream and the disk, and is aligned with the y axis in the radial direction and the z axis aligned vertically. Symmetry about the disk midplane is assumed. The inflow of the stream and disk are prescribed as boundary conditions, and the calculations are run until the mass and vertical kinetic energy within the box reach an approximate steady state. This requires ~ 2 flow crossing times of the grid. Gravity from the accreting star only is included. The grid covers 50 % of the

¹Permanent address: Canadian Institute for Theoretical Astrophysics, McLennan Labs, 60 St George St, Toronto, M5S 3H8, Canada

radius of the disk, and about 45° in azimuth.

The disk prior to impact with the stream is taken to be in hydrostatic equilibrium in the vertical direction, which together with an isothermal vertical structure corresponds to a gaussian density profile with scale height H_d . At the outer edge of the disk, R_{out} , the sound speed, c_s is set such that the Mach number of the flow is 30. The disk is always taken to be isothermal in the vertical direction, for most calculations we additionally assume that the disk is isothermal radially, so that $H_d(R) \propto R^{3/2}$. The flaring of the disk implied by this means that the strongest interaction with the overflowing gas will be near the disk rim.

Since the hydrodynamics of the impact are essentially those of hypersonic flow past an obstacle, the sharpness of the *radial* truncation of the disk at the outer edge may be expected to be of some importance. Tidal torques, and possibly the ram pressure of the stream itself, will tend to produce a sharp edge to the disk, but this will be opposed by the turbulent motions giving rise to the viscosity. Consequently, we assume a gaussian fall-off of the disk midplane density ρ_{d0} beyond R_{out} , with a scale length equal to the vertical scale height H_d . Interior to R_{out} the midplane density is constant with radius.

The initial conditions for the gas stream are similar to the results of the integration of the stream dynamics described by Lubow (1989). We assume that the stream density falls off with distance from the stream center as a gaussian, with scale length H_s , and central density ρ_{s0} . The initial vertical velocity is taken as $v_z \propto -z$, with the constant of proportionality equal to $0.6c_s$, implying modest convergence of streamlines towards the disk midplane. The Mach number of the stream at the disk edge is 30, and the angle between the stream and the radial direction at the impact point is 15° . The stream gas is taken to have the same temperature as the outer edge of the disk, for many systems this will be a reasonable assumption. In cases where the outer parts of the disk are much hotter than the surface layers of the secondary, ballistic stream overflow would of course be inhibited.

Slow inflow through a viscous disk implies that $\rho_{d0} \gg \rho_{s0}$. To within factors of order unity, a steady-state disk described by the Shakura-Sunyaev (1973) α -prescription for the viscosity has,

$$\frac{\rho_{s0}}{\rho_{d0}} \simeq 6\alpha \left(\frac{c_s}{v_s}\right) \left(\frac{H_d}{H_s}\right)^2, \quad (1)$$

with v_s the stream velocity at the impact point. For the parameters of our calculations, and assuming a typical α value of 0.1 for interacting binary disks, $\rho_{s0}/\rho_{d0} \sim 10^{-2}$, and we use this density ratio in the simulations.

Reflecting boundary conditions are imposed at the disk mid-plane, $z = 0$. Inflow boundary conditions are specified where the disk flows into the computational volume, at $x = 0$, and at $y = 0$ over the area where the stream enters. Over the remainder of the $y = 0$ plane, and for the other three faces of the computational box, outflow boundary conditions are used. Additionally, for the adiabatic simulations, we allow outflow through the $x = 0$ face where the calculated inflow density for the disk is below 10^{-12} of the central disk value (i.e. at high z). This is required in order to prevent artefacts arising near the boundary at

several scale heights above the disk midplane.

For reference, the calculations use second order (van Leer 1977) interpolation for all advected quantities, a dimensionless coefficient of artificial viscosity $C_2 = 2.0$, and a Courant number of 0.5.

2.2. Cooling

We have run simulations with three equations of state; isothermal, adiabatic (with no cooling), and one with optically thin radiative cooling included. The isothermal and adiabatic with no cooling cases bracket the range of possible behavior, the calculation including cooling is more realistic although there are many complexities that we do not attempt to model in these calculations.

If cooling is so rapid that the equation of state is effectively isothermal, then the main parameters of the problem as set up here are the Mach number of the flow, the ratio of disk to stream density, and the ratio of disk to stream scale heights. The results in this limit are independent of the absolute disk density, or equivalently of the mass transfer rate in the stream. This degeneracy is broken when more realistic cooling is included, dense gas then cools faster than diffuse material, and the results depend on the actual value of \dot{M} .

For a simple description (following Blondin, Richards & Malinowski 1995) the cooling time is given approximately by,

$$t_c \approx \frac{k_B T_{\text{gas}}}{n \Lambda(T_{\text{gas}})}, \quad (2)$$

where k_B is the Boltzmann constant, n is the number density of electrons, and Λ is the cooling rate in $\text{ergs cm}^{-3} \text{s}^{-1}$. We use for $\Lambda(T_{\text{gas}})$ the cooling function given by Dalgarno & McCray (1972, see also Cox & Daltabuit 1971), for which t_c (defined here as the time required to cool to $T_{\text{gas}}/2$) is given at a fiducial temperature of 10^6 K by,

$$t_c \simeq 10^2 \left(\frac{n}{10^{10} \text{cm}^{-3}}\right)^{-1} \text{ s}. \quad (3)$$

The qualitative hydrodynamics of the flow will then be determined (Blondin, Richards & Malinowski 1995) by the ratio of t_c to the dynamical time at the edge of the disk, $t_d \sim \Omega^{-1}$, where Ω is the Keplerian angular velocity. For many systems, t_d will be of order 10^3 s or longer.

For an estimate, we assume that the emission from the hotspot arises from material at comparable density to that in the stream (the post shock density will be higher than this, so cooling will be *more* rapid in the optically thin limit). Then to order of magnitude,

$$n \sim 2 \times 10^{12} \left(\frac{\dot{M}}{10^{-10} M_\odot \text{yr}^{-1}}\right) \left(\frac{H_s}{5 \times 10^9 \text{cm}}\right)^{-2} \times \left(\frac{v_s}{300 \text{kms}^{-1}}\right)^{-1} \text{ cm}^{-3}. \quad (4)$$

Comparison of this equation with equation (3) indicates that in the regime where optically thin cooling described by a cooling function is a valid approximation, typical accretion rates imply a cooling time $t_c \ll t_d$. Thus, at low accretion rates we expect the gross hydrodynamics of the stream-disk impact to be well described by an isothermal

equation of state. The flow may be expected to depart from isothermal behavior in the low density regions several scale heights from the midplane, and to explore this regime we have run several simulations including optically thin cooling.

2.3. Dependence of the effective equation of state on the accretion rate

The above argument suggests that the accretion rate will generally be high enough that cooling will be rapid, *provided* that the emission is optically thin. In this regime an isothermal equation of state should provide a good description of at least the higher density regions of the flow, within a few scale heights of the disk midplane. At higher accretion rates the assumption that the optical depth to the emitting regions of the hotspot is small will break down, and qualitatively we expect that the hydrodynamics will be better approximated by an adiabatic equation of state. As we demonstrate later, the flow in these two regimes is very different – here we estimate where the transition between them occurs.

The radiation emitted as the shocked stream gas cools must escape, at a minimum, through the hot ($\sim 10^6$ K) shocked layer and the relatively cool ($\sim 10^4$ K) inflowing stream material. We consider first the opacity due to the cooler stream. The temperature of the stream at the outer edge of the disk will be comparable to the surface temperature of the mass losing star, with a modest enhancement from compressional heating as the stream converges on the disk midplane (in some systems irradiation of the stream by the disk or hotspot might also be important – this would be particularly significant if the stream gas was able to be highly ionized prior to striking the disk). The dominant opacity source is therefore likely to be H^- scattering. An analytic approximation to the opacity in this temperature range is given by Bell & Lin (1994), in units of $\text{cm}^2 \text{g}^{-1}$,

$$\kappa = \kappa_0 \rho^{1/3} T^{10} \quad (5)$$

with $\kappa_0 = 10^{-36}$. The column density for escape of the hotspot radiation will evidently be $\sim \rho_{s0} H_s$, for which the optical depth is,

$$\tau \sim \frac{\kappa \dot{M}}{\pi H_s v_s}. \quad (6)$$

Imposing the condition that $\tau = 1$ then gives an estimate for the critical accretion rate for the transition between isothermal and adiabatic behavior. Using the numerical values adopted previously we obtain,

$$\begin{aligned} \dot{M}_{\text{crit}} \sim 2 \times 10^{-9} \left(\frac{H_s}{5 \times 10^9 \text{cm}} \right)^{5/4} \left(\frac{v_s}{300 \text{kms}^{-1}} \right) \\ \times \left(\frac{T}{10^4 \text{K}} \right)^{-7.5} M_{\odot} \text{yr}^{-1}. \end{aligned} \quad (7)$$

For accretion rates below this value cooling should be efficient, above it the radiation will be trapped by the inflowing stream gas and the initial cooling of the hot spot region will occur via adiabatic expansion.

The opacity of the hot shocked layer can also limit the applicability of the efficient cooling assumption. At \dot{M}_{crit} , the central stream density for the parameters used previously is $\sim 5 \times 10^{-11} \text{gcm}^{-3}$. While the shock is still

isothermal, the compression could be as large as the Mach number (~ 30) squared, giving a shocked layer with a density of $\sim 5 \times 10^{-8} \text{gcm}^{-3}$. For an opacity due to electron scattering, $\kappa = 0.348$, and $\tau = 1$ requires a thickness of the hot layer of order 10^8cm . As this is indeed roughly the thickness expected of the shocked region, it suggests that the critical accretion rate for the emission to become optically thick from the opacity of the shocked layer itself is comparable to, or somewhat less than, the critical value estimated above. We conclude that, with considerable uncertainties, both arguments give $\dot{M}_{\text{crit}} \sim 10^{-9} M_{\odot} \text{yr}^{-1}$.

Clearly the above analysis is extremely crude, and no substitute for a proper radiative transfer calculation of the hotspot region. *A priori* it would definitely be wise to keep an open mind as to whether a system with a given accretion rate would be better described theoretically with isothermal or adiabatic models. However it suggests that the hotspot region in low accretion rate cataclysmic variables might well be able to cool efficiently, whereas nova-like variables and supersoft X-ray sources with accretion rates much larger than \dot{M}_{crit} are almost certainly unable to do so.

In the following section we present models for both limiting cases. For low accretion rate systems we use an equation of state that is either isothermal, or which includes radiative cooling in the optically thin limit. These are qualitatively very similar, and differ mainly in the very low density regions where optically thin cooling becomes ineffectual. For models intended to represent better higher accretion rate systems we use an adiabatic equation of state without any cooling. Real systems, where cooling *will* occur in the low density parts of the flow, would be expected to have intermediate properties between the limiting extremes presented here.

2.4. Structure of the impact region for isothermal and adiabatic equations of state

Figure 1 (Plate XXX) illustrates the primary differences between the simulations using isothermal (or efficient radiative cooling) and adiabatic equations of state. The left panels show isodensity surfaces for an isothermal calculation, plotted at a density that is 10^{-3} of the central disk density, or 1/10 of the central stream density. The colors represent the radial velocity on this surface.

For this equation of state, the uppermost part of the stream where the density significantly exceeds that of the disk is able to flow smoothly over the rim of the disk in the manner envisaged by Lubow & Shu (1976), and Frank, King & Lasota (1987). We do not observe any instabilities that lead to rapid entrainment of the stream as it flows over the disk surface, though the leading edge of the stream is deflected by the ram pressure of the disk gas. More interestingly, there is a fairly broad region of the disk, downstream of the region where the stream is overflowing, which possesses significant inward velocity. This is material that has been brought to an intermediate velocity between that of the stream and the disk, as a result of the stream-disk interaction. In our simulations including radiative cooling this gas is hot, and thus a potential source of emission with a radial velocity that is highly supersonic, but less than that of the ballistic stream.

The right panels of the Figure show the results for an adiabatic equation of state. Here, the isodensity surface is plotted at a density that is $10^{-2.75}$ of the central disk density, and the colors represent $\log(c_s)$ on that surface. The details of this calculation will be discussed in Section 2.6, but it is obvious from the Figure that in this case the upper regions of the stream are *not* able to flow unimpeded over the surface of the disk. Rather, the qualitative impression is that the impact leads to a hot bulge extending along the rim of the disk. This material is not in hydrostatic equilibrium, and expands outwards downstream of the impact point. Material is still overflowing towards smaller radii, but it is not in the form of a coherent stream. We also note that even in the absence of radiative cooling, the temperature on the plotted surface declines rapidly (on the scale of a few H_s) moving downstream of the impact point.

2.5. Results for an isothermal equation of state / efficient radiative cooling

Figures 2 through 4 show in greater detail the results of the calculation that was illustrated in the left panels of Fig. 1. This employed an isothermal equation of state, and a ratio of stream to disk scale heights $H_s/H_d = 2$. The computational volume extended vertically to 5 disk scale heights, and in the x and y directions for 16 disk scale heights. We discuss later the differences in simulations including efficient radiative cooling, but the general behavior seen in those runs is the same as in the isothermal case. The computational grid used was $176 \times 176 \times 55$ cells. We have run simulations including radiative cooling at resolutions of up to $192^2 \times 60$, and adiabatic calculations at up to $128^2 \times 40$. We note, however, that there is a sharp vertical density gradient in the disk in the region, several scale heights above the midplane, where the stream is overflowing. Higher resolution might thus reveal additional interactions that are not resolved in these calculations.

Fig. 2 shows density contours and velocity vectors in the $x - y$ plane, with the stream entering from the bottom in each panel, and the disk gas flowing in from the left. In the disk midplane (top left panel), the stream is stopped rapidly at the edge of the disk by the much denser disk material. There is no ‘splashing’ or ricocheting material. Moving upwards, at around 2 disk scale heights above the midplane (top right panel) the densities of the stream and disk start to become comparable. Here we resolve the twin shocks in the disk and stream gas seen in earlier two dimensional calculations (Rozyczka & Schwarzenberg-Czerny 1987) and predicted analytically (e.g. Livio 1993). We also see that the velocity field of the disk gas downstream of the impact point has been disturbed by the impact – this material now has a significant radial velocity inward. At higher elevations the stream rapidly begins to dominate. At $z = 2.5H_d$ the stream is already able to penetrate to the inner boundary of the computation (at $\sim 0.5R_{\text{out}}$), and at $z = 3H_d$ the stream is overflowing almost freely, with some modest deflection of the edge facing the oncoming disk material.

Comparing these results with the two dimensional calculations of Rozyczka & Schwarzenberg-Czerny (1987), which have close to identical resolution in the plane, we see the same shock structure and some evidence of unstable flow in the mixed stream and disk layer. However our

3D simulations do not support the idea of a hotspot region that is highly extended along the disk rim. In our calculations shocks, and hence emission (given the implicit assumption of rapid cooling), are restricted in the midplane to the part of the disk directly struck by the stream. At higher z , the shocks are extended, but primarily along the radial direction. The two dimensional nature of earlier calculations, together with the assumption of a slow fall-off of the density at the disk edge, are likely to be responsible for these differences.

Fig. 3 shows density contours in a vertical slice taken along the initial stream flow direction. Although the stream is converging towards the disk midplane at all radii, the interaction between the stream and the disk is concentrated at the disk rim. Inward of the rim, there is a clear density minimum between the upper surface of the disk and the lower part of the overflowing stream. This is in accord with the prediction of Lubow (1989), and it suggests that the final fate of the stream, not modeled here, will be to reimpact the disk near to the point of the ballistic stream’s closest approach to the central object. We note that the separation between overflowing stream and disk seen in this simulation is accentuated by the strong flaring of the disk scale height implied by the isothermal assumption, $H_d \propto R^{3/2}$. However, weak interaction between stream and disk interior to the rim is also seen in a simulation where we took $H_d \propto R^{9/8}$, appropriate if the disk central temperature scales with the run of effective temperature $T_{\text{eff}} \propto R^{-3/4}$ (a ‘standard’ disk). Of course stronger interaction *would* be expected if the disk atmosphere was much more vertically extended than a gaussian.

Fig. 4 shows the density on vertical cylindrical surfaces at constant radii in the disk (i.e. the co-ordinates are $R\phi, z$). Three radii are depicted, at $R > R_{\text{out}}$, showing just the cross-section of the stream, at the disk rim where interaction is strongest, and where the stream is overflowing the disk interior to the rim. The distortion of the stream by the ram pressure of the disk can be seen, and it is clear that the main effect of the stream on the disk rim downstream of the impact point is to greatly reduce the density at high z . The stream acts as a windbreak in the flow, and truncates the disk in the vertical direction. For these parameters a very small quantity of disk gas is deflected *over* the stream – this phenomenon is stronger in simulations where radiative cooling is included and can lead to a hot wake of material downstream of the impact point along the rim.

These results are obtained for strictly isothermal flows. However, the flow in simulations including explicit radiative cooling is extremely similar in the regime where the cooling is much more rapid than the dynamical timescale. As argued earlier, this should be applicable to disks that are optically thin at all reasonable accretion rates.

Fig. 5 compares the results of the isothermal calculation with two simulations which include cooling. The cooling simulations assume central disk electron densities of 10^{14} and 10^{13} particles per cm^{-3} , which correspond to accretion rates of order 10^{-10} to $10^{-11} M_{\odot}\text{yr}^{-1}$. The cooling simulations used a $128^2 \times 40$ grid. A floor temperature of 10^4 K was imposed. We plot vertical profiles of density and, for the runs with cooling, temperature, at a point 20° downstream of the stream impact point just interior to the disk rim.

The density profiles show that the low density wake behind the overflowing stream persists in all three runs. In the runs incorporating cooling the density at high z can be two to three orders of magnitude higher than for the isothermal case – this is a consequence of the overspill of disk gas *above* the stream mentioned earlier. The absolute density though is very low in all cases. High temperatures of 10^5 K and above are seen in a layer above the disk surface, this is material that has been shock heated by the interaction with the stream and which has passed beneath the overflowing gas. This feature is not adequately resolved in these simulations.

2.6. Results for inefficient cooling

Fig. 6 summarizes the results for a simulation with an adiabatic equation of state and no radiative cooling. The grid was again $128^2 \times 40$ cells, and $H_s/H_d = 2$. The remaining initial conditions were as for the isothermal and radiative cooling runs, except that the stream injection point was moved slightly further from the $x = 0$ boundary in order to reduce effects arising from the finite volume of the computational box.

Qualitatively, the distinction from the isothermal calculations is that in this simulation the hot shock-heated gas expands in all directions and disrupts the coherent overflowing stream seen previously. In the disk midplane, ‘splashing’ of hot material downstream of the impact point is evident, though the velocities of this gas are substantially less than those of the disk. At $z = 3H_d$ there is overflow in a broad fan over the disk surface. Most of this material appears to be stream gas that has suffered a strong deflection upon reaching the disk edge, though an examination of the velocity field also shows disk material at high z that is being deflected inwards as a result of the stream interaction.

A slice along the initial stream flow direction now resolves clearly the shocks in the stream and disk gas. The overflowing component has a velocity that is predominantly in the $x - y$ plane, with a small (a few times c_s) vertical component. Further from the disk midplane significant vertical velocity away from the disk *is* seen, suggesting that with this equation of state a substantially greater absorption column will be generated for lines-of-sight well away from the disk plane. As shown later, the actual fraction of the stream overflowing the disk rim is comparable to that in the isothermal case, but the structure of the flow is here very distinct.

2.7. Global effects

The ZEUS simulations discussed in this paper suggest a picture in which efficient radiative cooling leads to a coherent stream overflowing the disk in a manner very similar to that described by Lubow (1989). Conversely, if cooling is inefficient, there is a ‘splashing’ of stream material off the disk edge. Similar quantities of material can flow inward in this regime, but there is no coherent stream and gas is also thrown outwards and upwards.

In order to examine the qualitative differences in global effects between the isothermal and inefficient cooling cases, we performed two three-dimensional smooth particle hydrodynamics (SPH) calculations. The results are shown in Fig. 7. These calculations have vastly lower resolution of the impact region than the ZEUS simulations, but

cover the whole disk and have been evolved for long enough (~ 10 binary orbits) to allow the disk to relax in the binary potential. We show an isothermal calculation (similar to that described in Armitage & Livio 1996), and a calculation with a polytropic equation of state ($\gamma = 1.1$) and system parameters appropriate to the supersoft source CAL87 (Callanan & Charles 1989; Gould 1995).

Similar features are evident in the SPH calculations as in the finite difference simulations. The isothermal run shows a narrow overflowing stream, while the polytropic calculation leads to a much more vertically extended spray of material and a bulge of outflowing gas near the impact point. Negligible masses of material escape the accreting star’s Roche lobe in either simulation. Although the choice of a value for γ in such a calculation is essentially arbitrary, it is clear from Figure 7 that the trend is such that systems where cooling is inefficient should display absorption at much higher elevations above the disk plane than those well described by an isothermal equation of state.

3. DEGREE OF STREAM OVERFLOW

To quantify the degree of stream overflow in the simulations, we compute the integrated radial mass flux through vertical $x - z$ slices which has a radial velocity $v_R \geq v_{\text{cut}}$. For $v_{\text{cut}} < 22c_s$ – the initial inflow velocity of the stream gas at the grid boundary – this quantity is conserved in the absence of interaction with the disk. Fig. 8 shows the radial mass flux as a function of R/R_{out} (where the R for each $x - z$ slice is evaluated along the line of the initial stream flow direction), for a variety of threshold radial velocities.

Outside the outer edge of the disk, all the curves coincide and are flat, reflecting steady-state undisturbed stream flow. For the runs with an isothermal or cooling equation of state, the amount of material flowing inward at the fastest velocity, $\geq 20c_s$, drops sharply as the disk rim is reached, and the central portions of the gas stream are stopped by the denser disk gas. In this case, and as noted previously, the main interaction occurs close to the disk rim, after which the highest velocity curve remains fairly flat at a lower level than initially. This mass flux is comprised of material that has overflowed the disk at large enough z to avoid strong interaction with the disk. For the illustrated case with $H_s/H_d = 2$, this is around 5% of the stream mass transfer rate.

From the Figure, it is evident that a significantly larger quantity of mass flows inward at velocities that are smaller than the ballistic stream velocity, but still highly supersonic. This is either stream material slowed by strong interaction with the disk, or disk gas entrained by the overflowing stream. For the case shown in Fig. 8, a radial mass flux of around 20% of the initial stream mass transfer rate is flowing inward with $v_R \geq 5c_s$ at the innermost boundary of the simulation volume, at $\sim 0.6 R_{\text{out}}$. We analyze the observational signatures of this material more fully in the following Section. We also note that close to the rim, the total mass of gas flowing inward supersonically exceeds the stream mass flux by a factor of $\sim 2 - 3$, though this does not extend far inward.

For the calculations with an adiabatic equation of state, and no cooling, the curves shown in Fig. 8 are different. In particular, there is a prominent dip in the curve with

the highest velocity cut near the outer rim of the disk, corresponding to the position of the shocks seen in Fig. 6. However, although the overflowing gas forms much less of a coherent stream in this case as compared to the isothermal simulations, the total mass moving inward is comparable. As with the calculation including cooling, around 10% of the stream mass flux overflows the disk at approximately ballistic velocities (although the stream is anything but ballistic in this limit), with substantially more gas flowing inward at lesser velocities.

For an estimate of the fraction of the stream mass transfer rate that overflows the disk, we assume that *all* the mass in the stream above some critical $z = z_{\text{crit}}$ manages to overflow the disk, while the stream below that height is stopped by the collision with the disk. For a simple approach, we take z_{crit} to scale with the height where the stream density equals that of the disk (e.g. Livio, Soker & Dgani 1986),

$$z_{\text{crit}} = \beta \frac{H_d H_s}{(H_s^2 - H_d^2)^{1/2}} \left(\ln \frac{\rho_{\text{d}0}}{\rho_{\text{s}0}} \right)^{1/2}, \quad (8)$$

where we have included a free parameter β as a scaling of this simple estimate.

Fig. 9 shows the results of 3 simulations, all incorporating radiative cooling, with varying ratios of stream to disk scale height. Points are plotted for three radial velocity cuts, together with a curve showing the fitting formula given in equation (8). As expected, the overflowing mass fraction is a strong function of H_s/H_d . For these parameters, $H_s/H_d = 1.5$ implies that only $\sim 2 \times 10^{-4}$ of the stream passes inward of the disk rim without strong interaction with the disk, although almost two orders of magnitude more material is moving inward at velocities greater than 5 times the sound speed. The naive fitting formula, with an appropriate choice of β (which is however close to unity), provides a good approximation to the simulation results.

4. VELOCITY MIXING BETWEEN STREAM AND DISK GAS

To quantify the observable effects of the stream-disk interaction on the velocity of the overflowing stream, we have computed the expected distribution of radial velocities, v_R , of gas along lines of sight to the central accreting object. We define the elevation angle of the line of sight to the disk midplane as θ , and consider viewing the system at a phase 18° downstream of the impact point (i.e along a diagonal line in Fig. 2 extending from the lower right corner towards the central object which is out of the frame beyond the upper left corner). We compare the results with those expected from a freely flowing stream in the absence of the interaction with a disk, obtained by running a simulation with the same stream initial conditions but no disk. This comparison calculation displays close to ballistic flow, but does include stream pressure effects. All the calculations in this Section used $H_s/H_d = 2.5$, so that a significant fraction of the stream overflows the disk rim.

Fig. 10a shows the results for an angle of elevation above the disk midplane of $\theta = 12^\circ$. This line of sight in the isothermal or cooling simulations probes freely overflowing gas at high z that has not undergone strong interaction with the disk. Consequently, we find that the radial velocity distribution is almost identical to that which would

arise from the same ballistic stream if the disk were absent. The distribution has a width of $\sim 5c_s$, with a sharp cut-off at large negative v_R .

Fig. 10b shows the results closer to the disk midplane, at $\theta = 9^\circ$. This line of sight probes gas which has had significant interaction with the disk. The interaction leads to reduced (less negative) radial velocities in the column of gas, corresponding to the ram pressure induced bending of the inner edge of the stream seen in Fig. 1, and a narrower distribution of v_R . The deviations from the ballistic prediction for the line of sight radial velocity are here at the $\sim 10\%$ level.

In general we find that for these relatively large angles above the disk midplane, the column of gas at large negative v_R greatly exceeds that of the undisturbed disk at $v_R \approx 0$. These velocity differences with the ballistic expectation are therefore potentially observable as absorption against the central object. For lines of sight that are closer to the disk midplane, we find gas with a range of radial velocities that become steadily closer to $v_R = 0$ as θ decreases. However, there is always a substantial component at $v_R = 0$ which arises from the undisturbed disk interior to the overflowing stream. This much lower velocity gas would therefore only be observable in emission.

Finally, we show in Fig. 10c the result for an adiabatic equation of state. As expected from the flow pattern seen in Fig. 6, the adiabatic equation of state leads both to a greater column of absorbing gas at high angles above the disk midplane, and a much larger spread of velocities of that gas. As compared to the isothermal simulations, the mean velocity of the gas along the line of sight is approximately halved, and there is a very broad spread of velocities extending even to positive v_R .

5. COMPARISON WITH OBSERVATIONS

Three classes of observations potentially probe the interactions modeled here: X-ray absorption ‘dips’ in nearly edge-on systems, which may track the column of overflowing gas; observations of the hotspot region where the shocks occur; and doppler tomography analyses which may be able to distinguish the velocities predicted to arise as a consequence of the stream impact. We briefly discuss these in turn.

Dips are seen in the UV and X-ray light curves of nearly edge-on low-mass X-ray binaries (LMXBs – e.g White, Nagase & Parmar 1995), intermediate polars, and dwarf novae (Long et al. 1996; Szkody et al. 1996). In the case of LMXBs, these have been interpreted as arising from the stream-disk interaction, either in the form of an overflowing component (Frank, King & Lasota 1987), or as a bulge excited on the rim of the disk (Hellier & Mason 1989; Mason 1989). Similar features seen in CVs also seem to be consistent with this interpretation. In particular, in Z Cha the dips in a UV lightcurve were seen to become shallower during the course of a superoutburst, which would be consistent with a declining mass transfer rate through the event (Harlaftis et al. 1992). For the dips observed in the intermediate polars FO Aqr, EX Hya, BG CMi and AO Psc, and in the dwarf nova U Gem in X-ray light curves (Hellier, Garlick & Mason 1993), the dips are observed to become shallower with decreasing orbital period of the systems. This is consistent with a statistically smaller mass

transfer rate in shorter period systems (e.g. Warner 1987; Patterson 1984), and an interpretation of the dips as arising from the stream-disk impact. It is also possibly fortuitous, as both the simulations and common sense suggest that the absorbing column should be a strong function of the system inclination. Moreover, these observations do not discriminate between the overflow and bulge models for the absorbing column, and there remains the observation of dips at a plethora of phases other than ~ 0.8 (e.g. Mason 1989; Thorstensen et al. 1991), where the impact occurs. Some of these may arise at the point where the stream converges and reimpacts the disk, which occurs at a binary phase of ~ 0.6 for a variety of mass ratios (Lubow 1989), or be generated due to an eccentric disk in low mass ratio systems. The latter possibility is suggested by the observations of Harlaftis et al., and supported by theoretical calculations (Whitehurst 1988a, 1988b; Lubow 1991, Armitage & Livio 1996; Murray 1996).

We also note that models for the structure of the accretion disk rim in supersoft X-ray sources require significant ‘splashing’ at the stream-disk impact point (Meyer-Hofmeister, Schandl & Meyer 1997). Since the accretion rates in these systems are extremely high ($\sim 10^{-7} M_{\odot} \text{yr}^{-1}$, e.g. van den Heuvel et al. 1992), this requirement is consistent with the results presented here. The effects of strong irradiation from the accreting object are an additional important complication in both these systems and in low-mass X-ray binaries (see, e.g. the simulations reported by Blondin 1997).

The simulations reported in this paper suggest that emission from the pair of shocks generated by the impact of the stream with the disk occurs over a smaller azimuthal extent than was implied by earlier calculations restricted to two dimensions. This is in general agreement with observations, for example of Z Cha, where Wood et al. (1986) obtain a hotspot extent of $\sim 4^{\circ}$ in azimuth, and IP Peg, where Wood & Crawford (1986) find an extent of $\sim 3-7^{\circ}$. The radially extended shock structure seen in the simulations is consistent with an apparently greater azimuthal extent of the hotspot when seen in ingress as compared to at egress, this is seen in IP Peg (Wood & Crawford 1986).

Optical spectroscopy provides a further probe of the absorption and emission expected to arise from an overflowing stream. For example, Hellier (1996) reports observations of the nova-like variable V1315 Aql. In this system, absorption that has been attributed to stream overflow is seen at phases close to the point where the stream impacts the disk. Further along the stream trajectory, emission is seen at velocities lower than the free-fall prediction. This would appear to be consistent with an approximately ballistic overflow model. However doppler mapping of another nova-like variable, SW Sex, shows emission that, if attributed to the stream-disk impact, seems more consistent with a bulge along the disk rim (Dhillon, Marsh & Jones 1997). This is also the interpretation advanced for doppler maps of the dwarf nova WZ Sge (Spruit & Rutten 1997), where the accretion rate is much lower.

Clearly, if the interpretation of all of these observations is correct, they do not fit nicely into the simple picture presented earlier, where the accretion rate determines the geometry of the stream overflow. However it is at least encouraging that observations, for example of OY Car (Billington et al. 1996; see also Bruch, Beele & Baptista

1996), may be capable of constraining the radial location of absorption features. This, together with theoretical predictions of the velocity fields arising from the stream-disk interaction, should help to disentangle the structure of the emission and absorption regions generated by the impact.

6. SUMMARY AND CONCLUSIONS

In this paper, we have discussed high resolution simulations of the stream-disk interaction in binary systems. We find as our main result that the qualitative behavior of the flow depends on the efficacy of cooling in the shock heated gas created by the impact. If cooling is efficient, specifically if the cooling time is much shorter than the dynamical timescale Ω^{-1} in the disk, then the upper reaches of the stream freely overflow the disk. This approximately ballistic flow is as described by earlier calculations (e.g. Frank, King & Lasota 1987; Lubow 1989), and is expected to terminate in a secondary hotspot where the stream reimpacts the disk close to its closest approach to the accreting object. We see no evidence for hydrodynamic instabilities leading to rapid entrainment of the entire stream as it flows over the disk. Additionally we find significantly larger quantities of mass that undergo strong interaction with the disk (or, are entrained disk gas), and flow inward with intermediate velocities. This gas may dominate the observed apparent velocity of the overflowing material at intermediate angles of disk inclination, and is likely to be visible in emission. We have argued that this efficient cooling mode of stream overflow is appropriate to CVs at low accretion rates, where the hotspot emission is emanating from regions that are not optically thick.

Conversely, if cooling is inefficient, then the interaction leads to a flow better envisaged as an explosion at the point where the stream impacts the disk (e.g. Livio, Soker & Dgani 1986). Material expands away from this point in all directions, and there is no coherent stream flow over the disk. Similar fractions of the incident gas stream flow inward in either regime, but in the case of inefficient cooling the impact leads to a more vertically extended ‘halo’ above and below the disk, and a bulge extending along the disk rim. The velocity of gas viewed along a line-of-sight to the accreting star displays a much greater dispersion in the case of inefficient cooling, and has a mean velocity that has a smaller magnitude than if cooling is efficient and the stream overflows ballistically.

Aside from the strength of cooling, the most important parameter in determining the degree of stream overflow is likely to be the ratio of stream to disk scale heights at the disk edge. We have quantified this for the case of efficient cooling. Assuming, as we have here, that both the stream and the disk have vertical density profiles that can be described as gaussians, then $H_s/H_d \gtrsim 2$ is required for significant stream overflow at ballistic velocities to occur (at lower ratios significant supersonic inflow at lesser velocities may still be produced). We find that the numerical results can be reasonably fit by a simple expression that assumes that the overflowing mass fraction scales with the fraction of the stream above the height where the disk and stream densities are equal.

The simulations reported here have used very simple isothermal vertical disk profiles, and this is probably the largest remaining uncertainty in the calculations. A density profile that declines markedly less steeply than the

isothermal one would lead to stronger interaction between the stream and the disk at several scale heights above the midplane. The observations discussed above suggest that overflow can occur in CVs, but in extreme cases such a density profile could inhibit overflow entirely. Even with weaker interactions, the influence of the stream on a disk wind or on large-scale magnetic structures anchored to the disk surface might extend the non-axisymmetric effects of the stream to larger elevations above the disk surface than

the purely hydrodynamic effects studied in this paper.

We thank Steve Lubow, Norm Murray and Paula Szkody for helpful discussions, and the referee for many helpful suggestions that improved the presentation of this work. P.J.A. thanks Space Telescope Science Institute for hospitality during the writing of this paper. M.L. acknowledges support from NASA Grant NAGW-2678.

REFERENCES

- Armitage, P. J., & Livio, M. 1996, *ApJ*, 470, 1024
 Billington, I., Marsh, T. R., Horne, K., Cheng, F. H., Thomas, G., Bruch, A., O'Donoghue, D., & Eracleous, M. 1996, *MNRAS*, 279, 1274
 Blondin, J. M. 1997, in *IAU Colloquium 165, Accretion Phenomena and Related Outflows*, eds. D. T. Wickramasinghe, L. Ferrario & G. V. Bickel, (San Francisco: ASP Conf. Ser.), in press
 Blondin, J. M., Richards, M. T., & Malinowski, M. L. 1995, *ApJ*, 445, 939
 Bruch, A., Beele, D., & Baptista, R. 1996, *A&A*, 306, 151
 Callanan, P. J., & Charles, P. A. 1989, in *Proc. 23rd ESLAB Symp. on Two-Topics in X-Ray Astronomy*, ESA SP-296, p. 139
 Clarke, D. A., Norman, M. L., & Fiedler, R. A. 1994, National Center for Supercomputing Applications Technical Report 015
 Cox, D. P., & Daltabuit, E. 1971, *ApJ*, 167, 113
 Dalgarno, A., & McCray, R. A. 1972, *ARAA*, 10, 375
 Dhillon, V. S., Marsh, T. R., & Jones, D. P. H. 1997, *MNRAS*, in press
 Frank, J., King, A. R., & Lasota, J. P. 1987, *A&A*, 178, 137
 Gould, A. 1995, *ApJ*, 452, 189
 Harlaftis, E. T., Hassall, B. J. M., Naylor, T., Charles, P. A., & Sonneborn, G. 1992, *MNRAS*, 257, 607
 Hellier, C. 1996, *ApJ*, 471, 949
 Hellier, C., Garlick, M. A., & Mason, K. O. 1993, *MNRAS*, 260, 299
 Hellier, C., & Mason, K. O. 1989, *MNRAS*, 239, 715
 Livio, M. 1993, in *Accretion Disks in Compact Stellar Systems*, ed. J. C. Wheeler (Singapore: World Scientific), p. 243
 Livio, M., Soker, N., & Dgani, R. 1986, *ApJ*, 305, 267
 Long, K. S., Mauche, C. W., Raymond, J. C., Szkody, P., & Mattei, J. A. 1996, *ApJ*, 469, 841
 Lubow, S. H. 1989, *ApJ*, 340, 1064
 Lubow, S. H. 1991, *ApJ*, 381, 268
 Lubow, S. H., & Shu, F. H. 1975, *ApJ*, 198, 383
 Lubow, S. H., & Shu, F. H. 1976, *ApJ*, 207, L53
 Mason, K. O. 1989, in *Proc. 23rd ESLAB Symp. on Two-Topics in X-Ray Astronomy*, ESA SP-296, p. 113
 Meyer-Hofmeister, E., Schandl, S., & Meyer, F. 1997, *A&A*, 321, 245
 Murray, J. R. 1996, *MNRAS*, 279, 402
 Patterson, J. 1984, *ApJS*, 54, 443
 Rozyczka, M. & Schwarzenberg-Czerny, A. 1987, *Acta Astron.*, 37, 141
 Shakura, N.I., & Sunyaev, R.A. 1973, *A&A*, 24, 337
 Spruit, H. C., & Rutten, R. G. M. 1997, *A&A*, preprint
 Stone, J. M., & Norman, M. L. 1992a, *ApJS*, 80, 791
 Stone, J. M., & Norman, M. L. 1992b, *ApJS*, 80, 819
 Szkody, P., Long, K. S., Sion, E. M., & Raymond, J. C. 1996, *ApJ*, 469, 834
 Thorstensen, J. R., Ringwald, F. A., Wade, R. A., Schmidt, G. D., & Norsworthy, J. E. 1991, *AJ*, 102, 272
 van den Heuvel, E. P. J., Bhattacharya, D., Nomoto, K., & Rappaport, S. A. 1992, *A&A*, 262, 97
 van Leer, B. 1977, *J. Comp. Phys.*, 23, 276
 Warner, M. 1987, *MNRAS*, 227, 23
 White, N. E., Nagase, F., & Parmar, A. N. 1995, in *X-Ray Binaries*, eds. W. H. G. Lewin, J. van Paralijs, & E. P. J. van den Heuvel (Cambridge: Cambridge University Press), p. 1
 Whitehurst, R. 1988a, *MNRAS*, 232, 35
 Whitehurst, R. 1988b, *MNRAS*, 233, 529
 Wood, J., & Crawford, C. S. 1986, *MNRAS*, 222, 645
 Wood, J., Horne, K., Berriman, G., Wade, R., O'Donoghue, D., & Warner, B. 1986, *MNRAS*, 219, 629

FIG. 1.— Isodensity surfaces from the isothermal (left column) and adiabatic (right column) simulations. The upper panels show the top view, with the stream flowing left to right and the disk flowing downwards; the lower panels show side views in which the disk material is moving out of the plane of the paper. The isothermal calculation is rendered at a density surface that is 10^{-3} of the central disk density. The adiabatic run is rendered at a density surface that is $10^{-2.75}$ of the central disk density. *This figure available as a jpeg in the astro-ph version. Interactive viewing of the simulations at http://www.cita.utoronto.ca/~armitage/hydro_abs.html.*

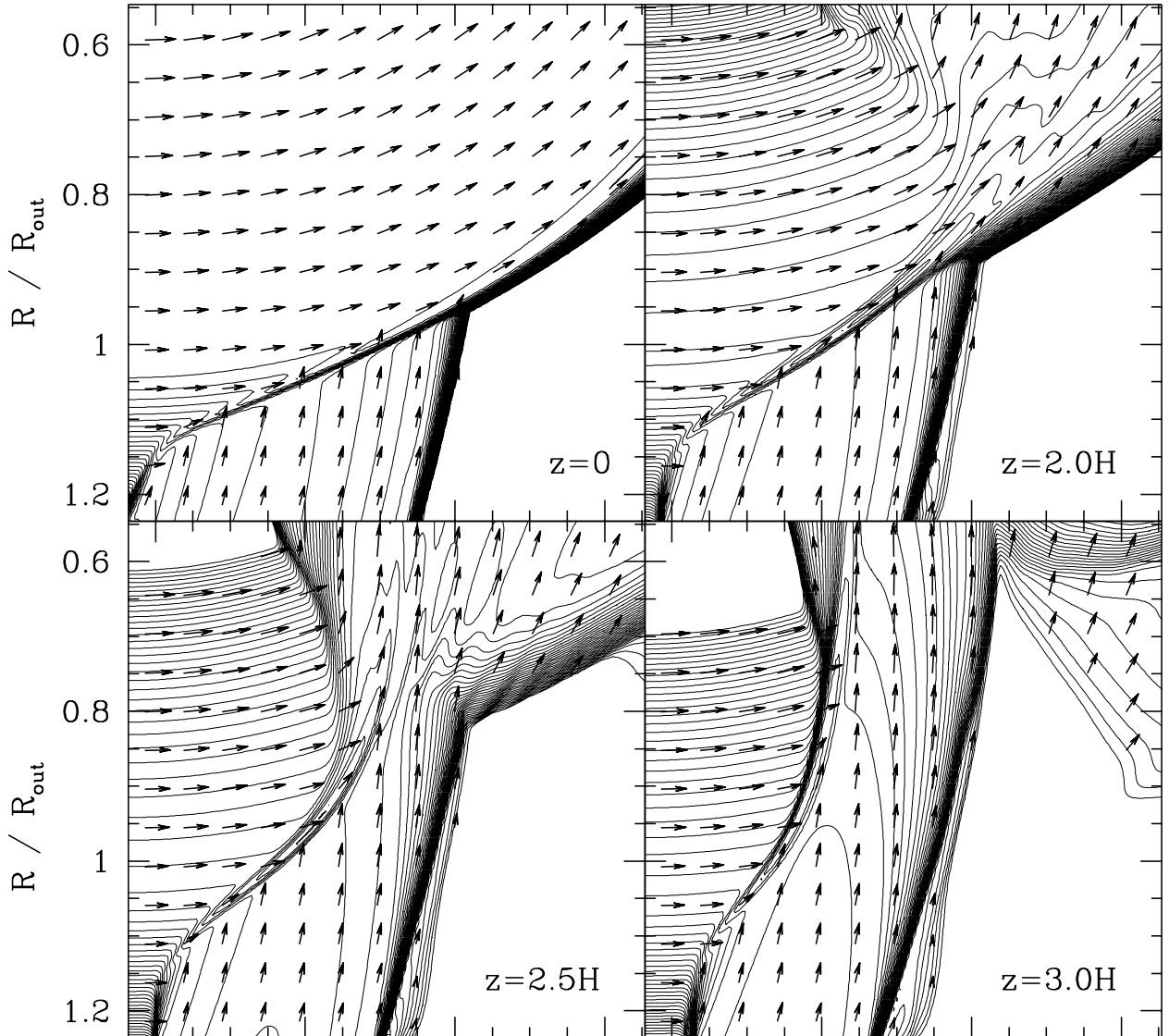


FIG. 2.— Density contours in the $x-y$ plane for a calculation with an isothermal equation of state. The computational grid was $176 \times 176 \times 55$ cells. $H_s/H_d = 2$. The panels depict slices in the disk midplane ($z = 0$), and at 2, 2.5 and 3 *disk* scale heights above the plane. The stream enters from the bottom in each panel, the disk flow is left to right. Contour levels are at $\Delta \log \rho = 0.3$, between $\log \rho = 0$ and $\log \rho = -12$. Arrows depict the direction and relative magnitude of the velocity field in each plane. The radius as a fraction of the disk radius R_{out} is also shown.

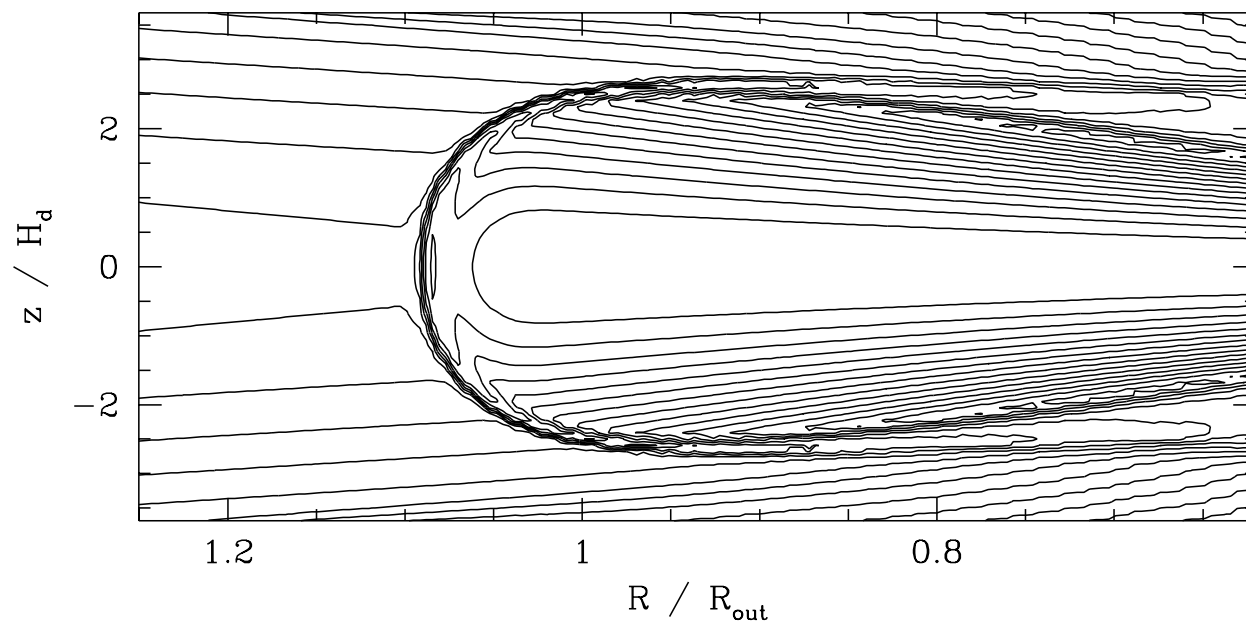


FIG. 3.— Density contours in a vertical slice along the initial stream flow direction for the isothermal calculation. Contour levels are at $\Delta \log \rho = 0.3$.

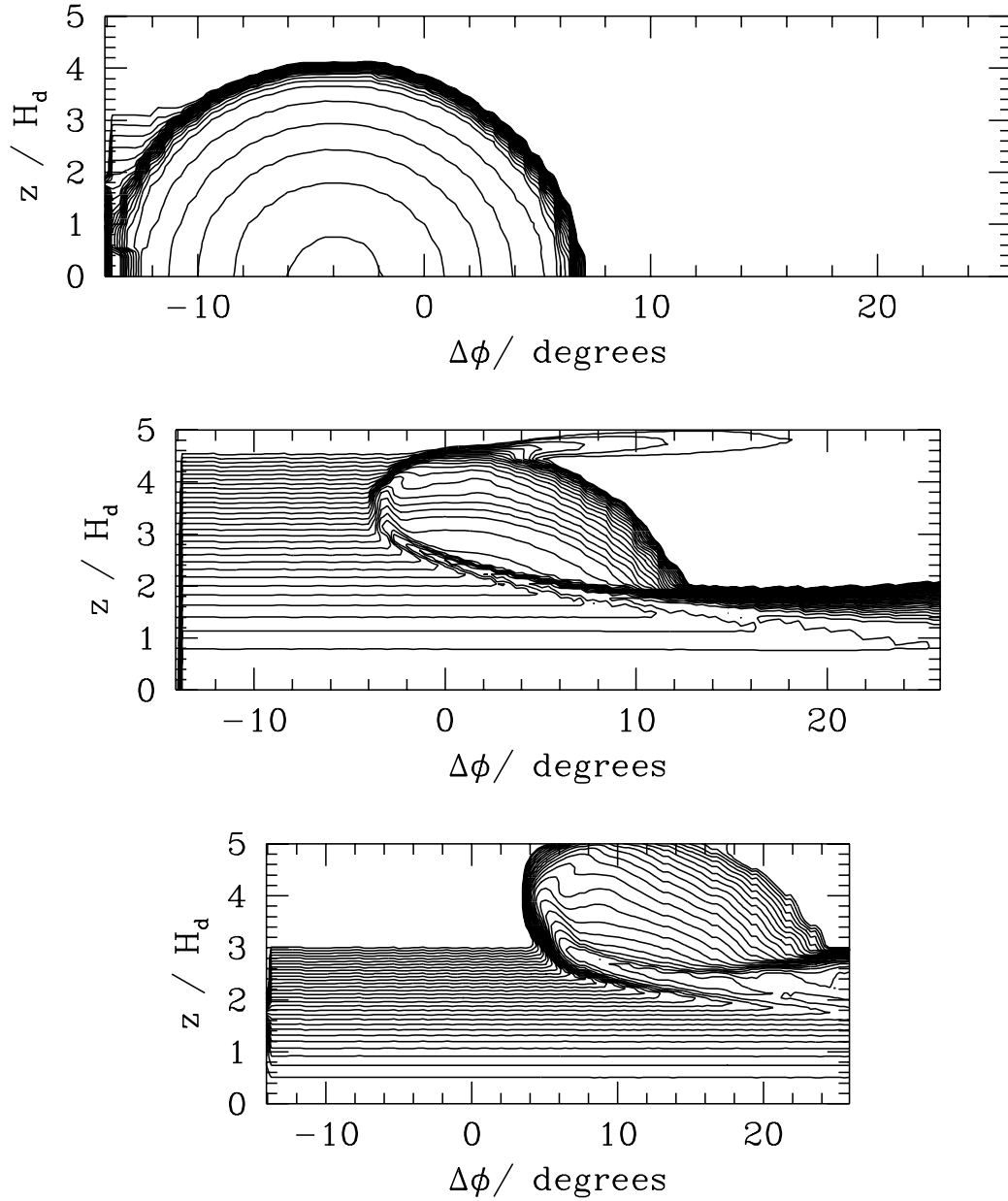


FIG. 4.— Density contours on cylindrical surfaces at constant radius from the accreting object ($R\phi, z$ surfaces). From top downwards, the surfaces are at radii of $1.2R_{\text{out}}$, $1.0R_{\text{out}}$ and $0.75R_{\text{out}}$. Contour levels are at $\Delta \log \rho = 0.3$, between $\log \rho = 0$ and $\log \rho = -9$. The x -axis is labelled with the angular distance relative to where the stream meets the disk edge – in this figure positive $\Delta\phi$ implies *downstream* of the impact point.

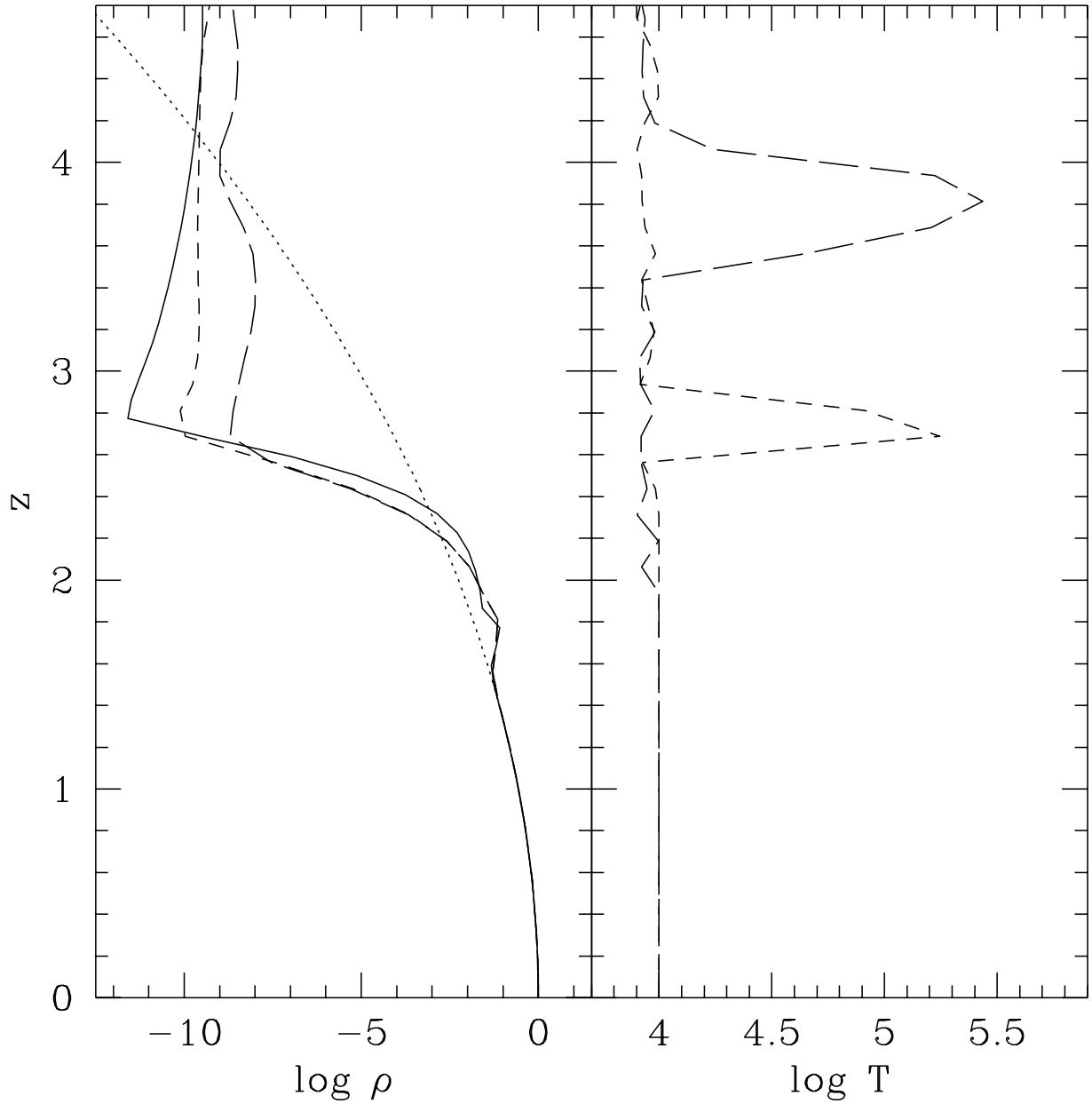


FIG. 5.— Illustration of the influence of the cooling rate on the vertical density and temperature profile downstream of the impact point on the disk rim (at $R = 0.9R_{\text{out}}$, and 20° downstream of the stream impact position). The solid line shows the result for an isothermal equation of state, the short dashed and long dashed lines for calculations including radiative cooling with central disk densities of 10^{14}cm^{-3} and 10^{13}cm^{-3} respectively. The dotted line in the density profile depicts the hydrostatic fall-off of density with height.

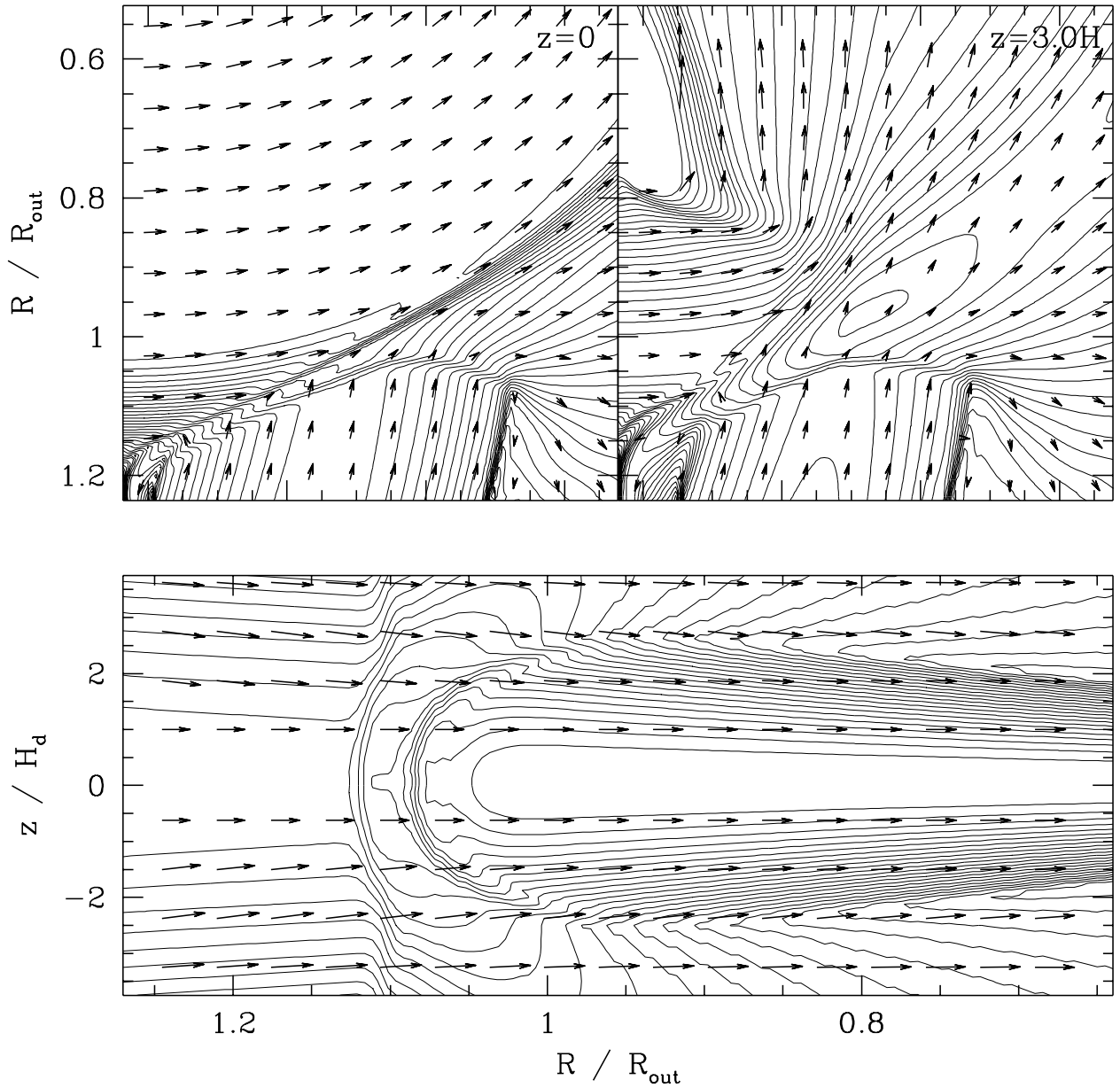


FIG. 6.— Summary of results for an adiabatic equation of state, with initial conditions corresponding to the isothermal calculation. The computational grid was $128 \times 128 \times 40$ cells. The upper panels show density contours in the $x - y$ plane at $z = 0$ and at 3 disk scale heights, the lower panel a vertical slice along the initial stream flow direction. Contour levels are at $\Delta \log \rho = 0.2$. Arrows depict the direction and relative magnitude of the velocity field in each plane. Note that the vertical slice is not in the radial direction, this is why there are non-zero velocities even within the disk material.

FIG. 7.— Results from SPH calculations of the entire disk with varying polytropic equations of state. Plotted is a side view of the system with the stream entering from the left. Upper panel is for an isothermal equation of state, lower panel from a calculation with $\gamma = 1.1$. Omitted for reasons of space. Armitage & Livio (1996) shows a similar figure.

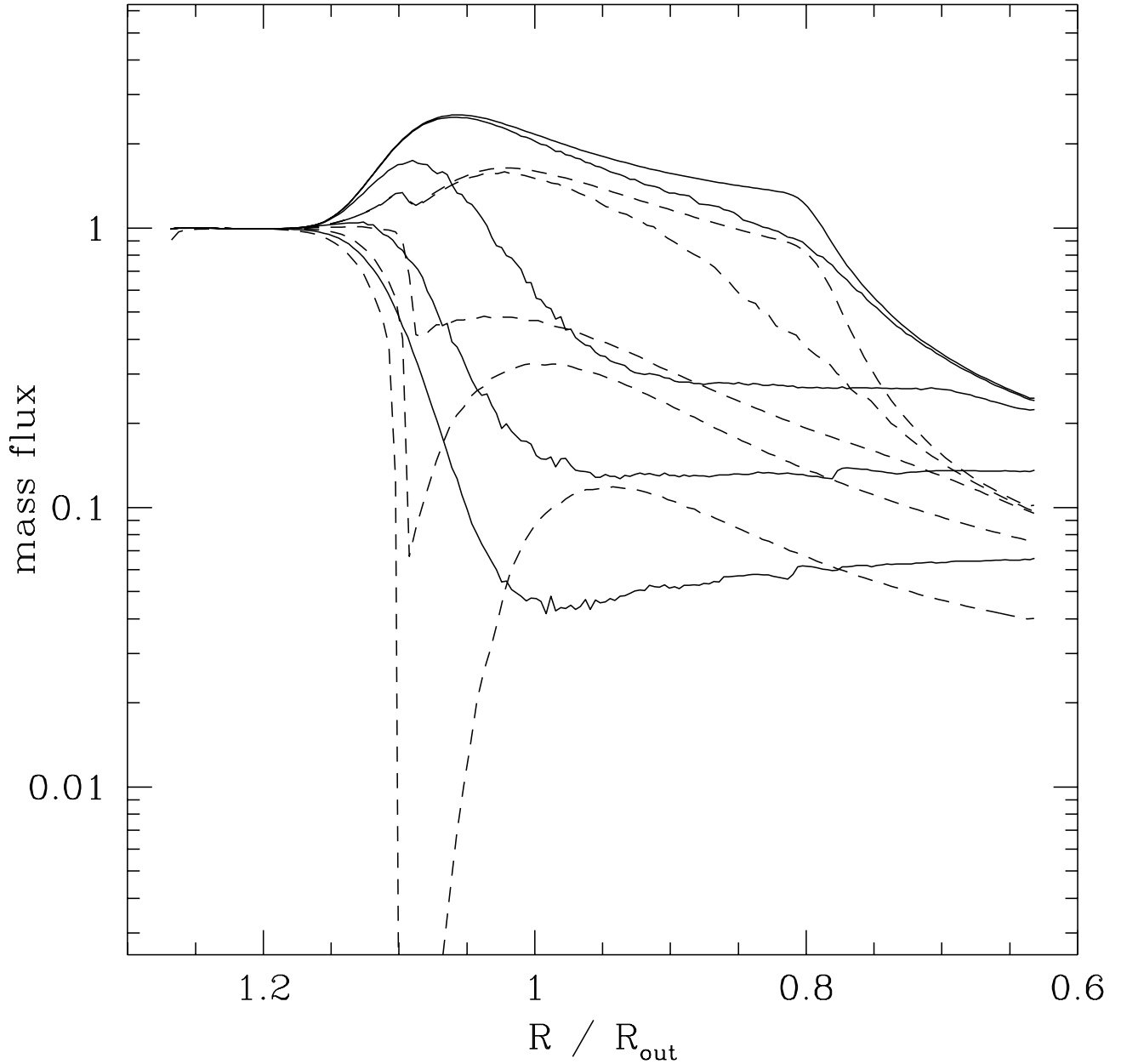


FIG. 8.— Mass flux with inward radial velocity $v_R \geq v_{\text{cut}}$ through vertical slices at varying y (labelled with the fractional radius R/R_{out} measured along the initial stream flow direction). The solid lines show the results from an isothermal simulation, The dashed lines are for an adiabatic calculation. Both simulations have $H_s/H_d = 2$. From top downwards, $v_{\text{cut}} = 0, c_s, 5c_s, 10c_s$ and $20c_s$.

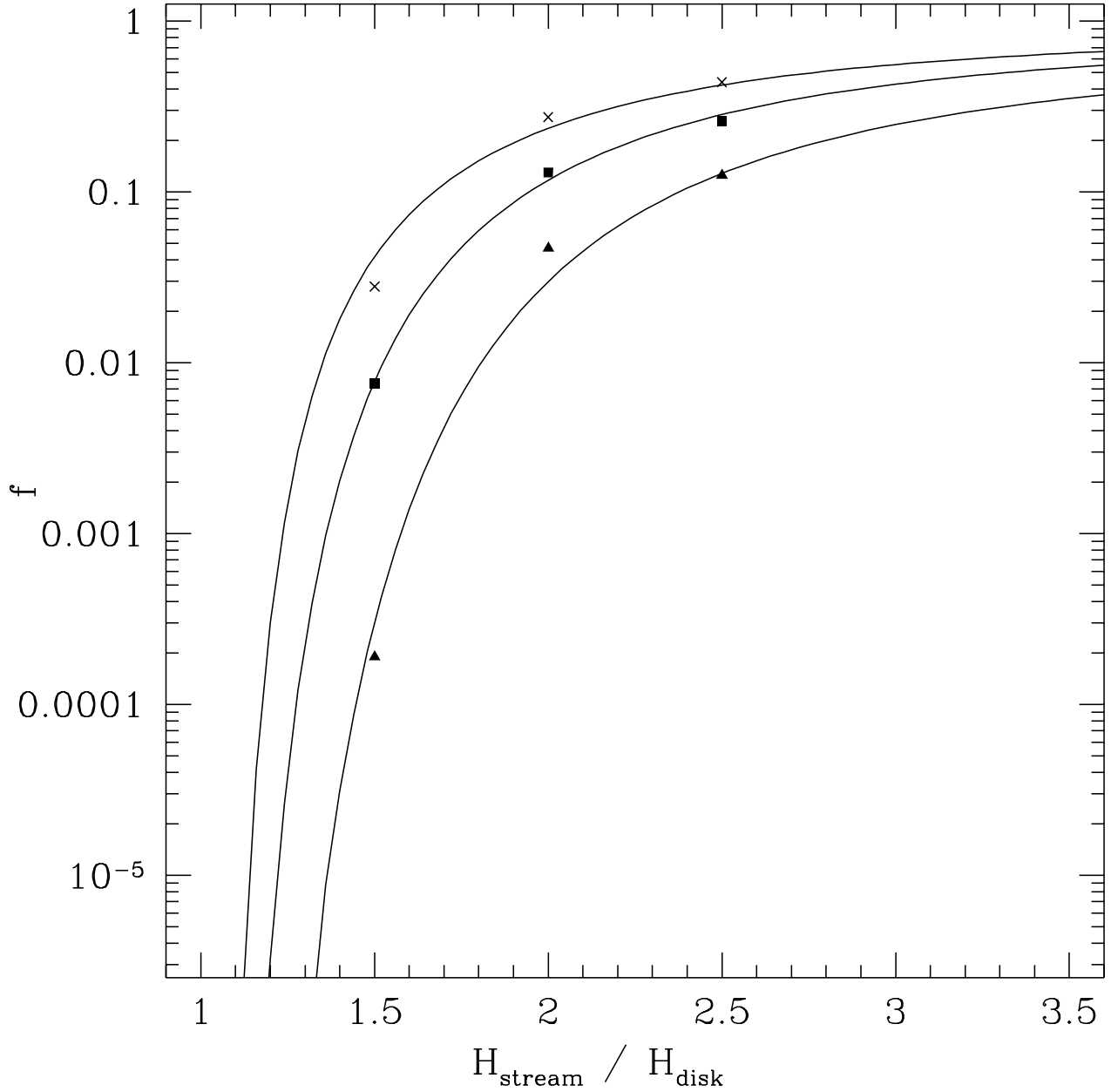


FIG. 9.— Overflowing mass as a fraction f of the stream mass flux, as a function of the ratio of scale heights of the stream to the disk $H_{\text{stream}}/H_{\text{disk}}$. The symbols are from the numerical simulations; crosses for mass inflow at $v_R \geq 5c_s$, squares for $v_R \geq 10c_s$, and triangles for $v_R \geq 20c_s$. The curves represent the scaling function described in the text, with $\beta = 0.85, 1.1$ and 1.5 respectively.

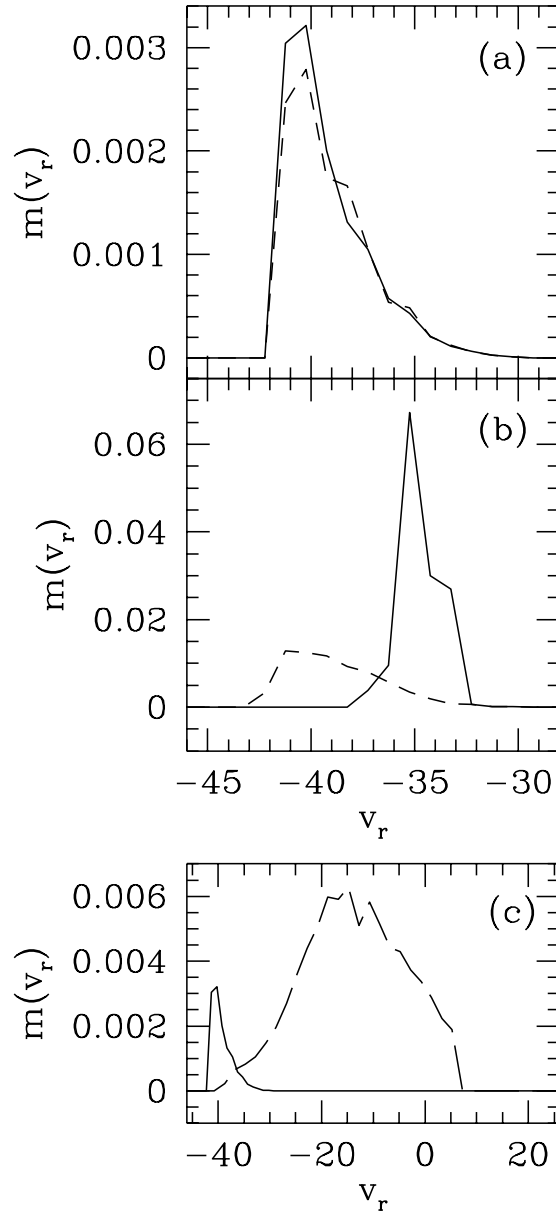


FIG. 10.— The radial velocity distribution of gas along lines of sight to the central accreting object. All panels are for a line of sight situated 18° downstream of the impact point. (a) Elevation angle above the midplane $\theta = 12^\circ$. Solid line is the result from a simulation including cooling, dashed line is the contribution from a ballistic stream with no disk interaction. (b) As in the previous panel except with $\theta = 9^\circ$. (c) Comparison of an adiabatic (long dashed line) simulation with a simulation including efficient cooling (solid line), for $\theta = 12^\circ$ (note different scale on the x axis).

This figure "hydro.jpg" is available in "jpg" format from:

<http://arxiv.org/ps/astro-ph/9709035v1>